

Contrastive Sequential-Diffusion Learning:

An approach to Multi-Scene Instructional Video Synthesis

Vasco Ramos¹, Yonatan Bitton², Michal Yarom², Idan Szpektor², Joao Magalhaes¹

¹NOVA LINCS, NOVA School of Science and Technology, Portugal,

²Google Research

Abstract

Action-centric sequence descriptions like recipe instructions and do-it-yourself projects include non-linear patterns in which the next step may require to be visually consistent not on the immediate previous step but on earlier steps. Current video synthesis approaches fail to generate consistent multi-scene videos for such task descriptions. We propose a contrastive sequential video diffusion method that selects the most suitable previously generated scene to guide and condition the denoising process of the next scene. The result is a multi-scene video that is grounded in the scene descriptions and coherent w.r.t the scenes that require consistent visualisation. Our experiments with real-world data demonstrate the practicality and improved consistency of our model compared to prior work.

1 Introduction

When people perform a task with numerous intricate steps, complementing the textual step instructions with visuals enhances user experience (Grafoni, 2009; Serafini, 2014). Indeed, many sites offer multi-scene videos to convey instructional textual descriptions, such as recipe instructions and do-it-yourself (DIY) projects (Lin et al., 2020).

State-of-the-art video synthesis methods (Ho et al., 2022; Singer et al., 2023; Wang et al., 2023b; Blattmann et al., 2023a,b) demonstrate remarkable performance in generating single-scene videos. Yet, only a few works address multi-scene video generation (Long et al., 2024; Lin et al., 2023; Yuan et al., 2024). These methods are focused on domains in which one single (typically human) character is the center of all scenes and achieve coherence by reusing and combining visual elements frame to frame. However, multi-scene instructional video synthesis raises a number of challenges. First, the input is a *strict sequence of actions*, for which there's a need to *generate the full sequence of*

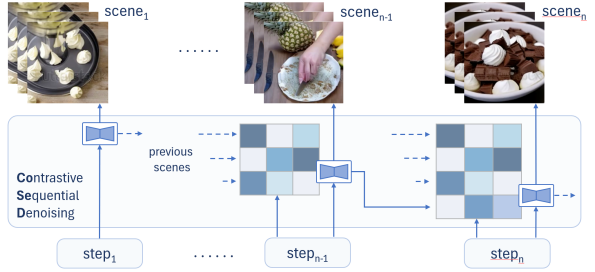


Figure 1: Contrastive sequential diffusion denoising (CoSeD) is grounded on an input sequence of step actions to synthesize multi-scene instructional videos. (Code and data will be available after publication)

videos. A model should not generate just the last scene, like (Koh et al., 2023), and one cannot provide the topic and let the model generate a random sequence of text-video pairs similarly to (Ge et al., 2023). Second, similar to story generation (Pan et al., 2022; Feng et al., 2023; Rahman et al., 2023; Maharana et al., 2022), the generative model needs to *determine which previous step in the sequence to ground each new scene to*. Third, while existing methods are focused on video generation in which one single (typically human) character is the center of all scenes (Long et al., 2024; Lin et al., 2023; Yuan et al., 2024), instructional videos typically incorporate multiple objects instead of central characters. Hence, we argue that multi-scene instructional video synthesis requires an approach that is sequence-grounded by design, (see Figure 1).

To this end, we propose CoSeD (Contrastive Sequential Diffusion learning), a model that addresses the above challenges with three key novelties: (1) to the best of our knowledge, we are the first to address the problem of multi-scene instructional video generation; (2) we introduce contrastive-diffusion-learning over latents sampled from previous generations; and (3) we contribute to understanding the role of seeds and conditioned latents in the reverse diffusion process. These advancements offer new perspectives and methods

that could significantly impact future research and applications in the field. Additionally, the compact size of our model facilitates efficient training, enabling fine-tuning for specific types of videos.

Experimentally, CoSeD demonstrates the capability to generate coherent sequences of videos across a wide range of instructional content, where strict alignment between language and vision is critical. The results show that CoSeD maintains high fidelity and relevance in video sequences.

2 Related Work

Various approaches have been explored to address coherence in image generation. Pan et al. (2022) proposes a history-aware autoregressive latent diffusion model, encoding the history of caption-image pairs into a multimodal representation. However, its computational complexity poses challenges. (Rahman et al., 2023) incorporates the complete history of U-net latent vectors, which can introduce noise. (Koh et al., 2023) fuses frozen text-only LLMs with pre-trained image encoder and decoder models through a mapping network, enabling multimodal capabilities like image retrieval and generation. However, this can break coherence if retrieved images don't align with the context. (Ge et al., 2023) integrates a visual tokenizer with a multimodal LLM to process text and images, excelling in multi-turn generation, but struggles with maintaining narrative coherence in story generation tasks.

To generate long single-scene videos (Blattmann et al., 2023b; Yin et al., 2023) generate sparse key frames and interpolates intermediary frames between them recursively to enhance the frame rate. Extending this idea, Blattmann et al. (2023a) implements meticulous data curation techniques, creating a large dataset of annotated video clips and filtering out those with low motion or excessive text. By contrast, (Bar-Tal et al., 2024) generates the entire video in a single pass, eliminating the need for sparse key frames and interpolation.

Advancements have also been made in generating coherent multi-scene videos. (Long et al., 2024) combines language, image, and video generation models using brute-force LLM prompting to create distinct scenes and detailed descriptions for each element. These are visualized using a text-to-image model, combined with scene descriptions, and passed to an image-to-video model for a coherent visual representation. Similarly, (Lin

et al., 2023) employs a two-stage process where GPT-4 (OpenAI, 2023) expands text prompts into detailed descriptions and ensures visual continuity by generating textual descriptions and entity layouts. (Yuan et al., 2024) introduces a multi-agent framework, breaking down tasks into sub-tasks, refining prompts, and generating images to create small video segments, which are then assembled into a final coherent video, achieving performance comparable to closed-source models. (Zhou et al., 2024) maintains coherence across frames using a Self-Attention mechanism and a module for smooth transitions, ensuring videos faithfully depict the input text's content. Lastly, (Bansal et al., 2024) enhances text-to-video (T2V) models by improving temporal alignment between video scenes and text segments, significantly enhancing visual fidelity and narrative coherence.

3 Contrastive Sequential Diffusion

Given a set of tasks, $\mathcal{D} = \{T_1, T_2, \dots\}$, where each task T_j comprises a sequence $T_j = \{s_{j_1}, \dots, s_{j_n}\}$ of step-by-step text instructions, our goal is to synthesize the sequence of scenes $V_j = \{v_{j_1}, \dots, v_{j_n}\}$ that is best aligned with the corresponding stepactions and all previous visual scenes. The result is a multi-scene video that depicts the steps of the task comprehensively and consistently across all scenes. For simplicity, we will omit the task index j from our notation.

In our setting, we depart from the linear dependency assumption used by previous works (Yuan et al., 2024) and acknowledge the possibility of a more complex and non-linear sequential structure (Donatelli et al., 2021). To address this assumption, the model must consider not only the current step s_n but also the pairs of previous steps and visual scenes $\{(s_1, v_1), \dots, (s_{n-1}, v_{n-1})\}$. This ensures coherence in the generated visual elements, maintaining consistency and accurately reflecting task progression, even in cases where individual steps are ambiguous or lack explicit information.

3.1 Sequential Diffusion

Latent Diffusion Models are designed to synthesize one single image or video at a time. Our goal is to move beyond this limitation and propose a sequential-diffusion models that contrastively learns how semantic and visual dependencies should exist in a sequence of multiple-scenes. Using the Latent Diffusion Models formulation pro-

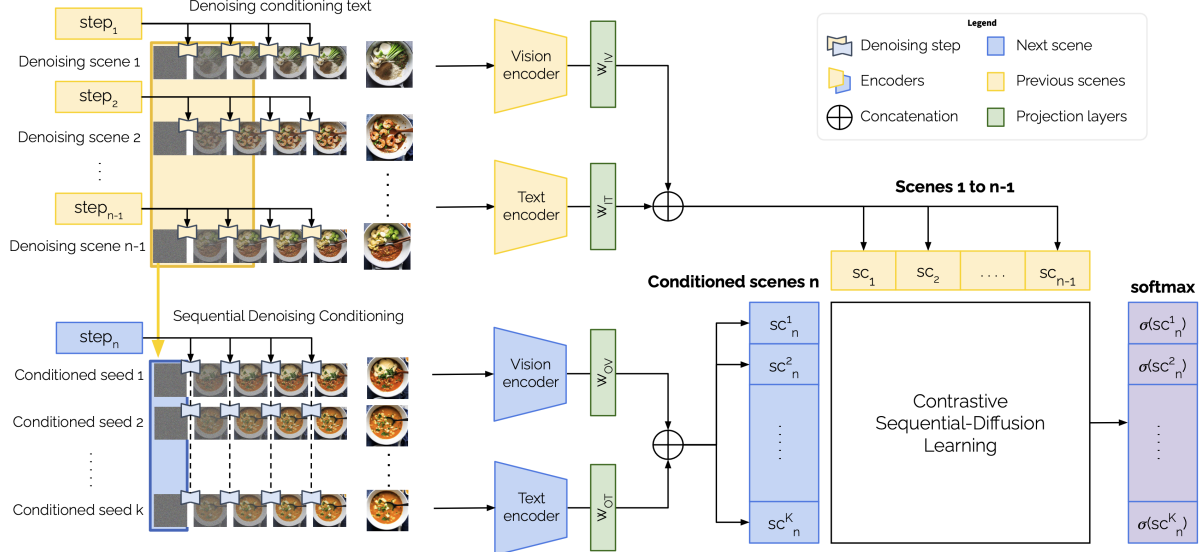


Figure 2: The proposed contrastive denoising diffusion learning architecture. The contrastive learning component learns the temporal relations which relations should exist between

posed by [Rombach et al. \(2022\)](#), the independent denoising process for each isolated step s_n of a sequence, is the direct application of the model,

$$\mathcal{L}_{LDM} = \mathbb{E}_{z_t^n, s_n, \epsilon, t} \left[\|\epsilon - \epsilon_\theta(z_t^n, t, \tau_\theta(s_n))\|_2^2 \right] \quad (1)$$

where z_t^n corresponds to the denoising iteration t of the visual scene v_n , hence $z_0^n = E(v_n)$. Formally, we wish to learn a sequence model that iterative estimates the v_n scene that maximizes the likelihood of the entire sequence of all previous $n - 1$ steps, $s_{<1}$,

$$\sum_{n=2}^N p(v_n | s_n, (s_{n-1}, v_{n-1}), \dots, (s_1, v_1)), \quad (2)$$

where N is the total number of step-actions in a given sequence. We propose to ensure the sequential consistency through the text conditioning encoder $\tau_\theta(s_i)$ and the visual denoising seed z_T^n . The proposed contrastive sequential-diffusion learning, Figure 2, addresses these two intuitions and will be discussed in next sections.

3.2 Sequential Language Conditioning

Following the work of [\(Bordalo et al., 2024\)](#) we use an LLM to transform the sequence of text steps-actions into visual captions. This has shown to produce LDM prompts that are visually richer, leading to better results.

Therefore, we train a decoder model φ to convert the entire context into one self-contained description,

$$\varphi(s_n | \{s_{n-1}, \dots, s_1\}). \quad (3)$$

This transformation will then condition the denoising process on the entire sequence of actions, leading to the loss function

$$\mathcal{L}_{CoSeD} = \mathbb{E}_{z_t^n, s_n, \epsilon, t} \left[\|\epsilon - \epsilon_\theta(z_t^n, t, c_n)\|_2^2 \right], \quad (4)$$

where $c_n = \tau_\theta(\varphi(s_i | s_{<i}))$ is the conditioning embedding vector that is inputted into the cross-attention of the U-Net ϵ_θ . Hence, on each denoising iteration t , the U-Net is now conditioned on an accurate visual depiction of the sequence context until step n .

3.3 Sequential Denoising Conditioning

In the previous section, we discussed the sequential dependency assumption $s_n | s_{n-1}, \dots, s_1$ for the denoising process input. However, achieving sequential dependency within the denoising process itself poses a challenge. While aligning the input description with the desired output enhances the final result, it does not inherently enforce the generation of visually consistent images. This can lead to accurate depictions of steps but without visual coherence. Therefore, guiding the denoising process is essential to ensure visual coherence across sequential outputs.

[Pan et al. \(2022\)](#), incorporate information from previous steps into the cross-attention mechanism inside the diffusion model to guide the generation. The drawback is that passing all information to the diffusion model requires intensive training and may overwhelm the generation with unnecessary data.

In the previous section, we mitigated this problem by using an external text model. [Rahman et al. \(2023\)](#) used all latent variables to create a vector for conditioning the generation process. However, including all latents in the conditioning process introduce noise, resulting in content generation based on irrelevant information from previous steps. In contrast, [Yuan et al. \(2024\)](#) adopt the approach of using only the last frame of the previous clip to initiate the generation of the next one. However, this approach encounters challenges when the current step is not directly dependent on the previous one. Therefore, we argue that relying solely on the last frame or all past latents may be suboptimal in non-linear scenarios.

Informed by previous works, we propose a contrastive method to learn which information should be selected from the past $(n - 1)$ denoising processes and included in the current denoising process n . This selective approach best approximates the non-linear nature of steps in a task that we aim to capture. Formally, the denoising iterations follow equation 4, except for the starting iteration T of the reverse diffusion process,

$$\mathcal{L}_{CoSeD} = \mathbb{E}_{z_T^n, s_n, \epsilon, t=T} \left[\|\epsilon - \epsilon_\theta(z_T^n, c_n)\|_2^2 \right], \quad (5)$$

where instead of having $z_T^i \sim \mathcal{N}(\mu, \sigma^2)$, we propose to sample denoised latents from previous steps of the sequence. Formally, z_N^T will be sampled from a set of past denoised latents,

$$z_T^n \sim \{z_T^{<n}, z_{T-1}^{<n}, \dots, z_{T-w}^{<n}\}, \quad (6)$$

where for each step n we consider all $(n - 1)$ steps and the first w denoising iterations. Finally, each candidate visual scene v_n^i is then computed with multiple denoising processes using the seeds $\{z_T^{<n}, z_{T-1}^{<n}, \dots, z_{T-w}^{<n}\}$. Hence, by conditioning the n generation process on latents from all steps in a nonlinear way, we enhance coherence in the generated data. This approach not only facilitates the selection of the most suitable information for each step, but also promotes coherence and continuity throughout the entire generation process.

3.4 Text and Vision Scene Embeddings

To effectively handle the text and visual modalities of a scene (s_n, v_n) in a sequence, we encode both modalities using CLIP ([Radford et al., 2021](#)), see Figure 2. Subsequently, the output of each encoder is reduced by half using linear projection layers.

We utilize two distinct weight matrices, one for text embedding and another for visual embedding the projected embeddings are then concatenated into one single vector. In addition to the projection layers per modality, we distinguish between the projections of past scenes from the projections of the current scene, which leads to four weight matrices $\{W_{IT}, W_{IV}, W_{OT}, W_{OT}\}$.

The embedding projections sc_n^i of all candidate scenes (s_n, v_n^i) and all past scenes $sc_{<n}$, allows us to represented all scenes in one single common embedding space.

3.5 Contrastive Classification

Given the result of the different denoising processes, v_n^i , we consider the candidate scene embedding sc_n^i and seek to identify the one that is best related to the context scenes. This decision is rooted in the need to avoid relying solely on the last scene due to concerns related to non-linearity. Our proposed approach prioritizes selecting the most accurate visual representation related to a determined task. The softmax function in Figure 2, is the ideal solution to infer the likelihood of each scene and select the one that maximizes it,

$$\arg \max_{v_n^i} \sigma_{CoSeD}(sc_n^i, sc_{<n}). \quad (7)$$

This approach leverages contrastive learning models ([Radford et al., 2021](#)), recasting them into a framework for contrastive selection within a sequential denoising process. Expanding the softmax operation,

$$\arg \max_{v_n^i} \frac{\exp(\sum_{k=1}^{n-1} sc_n^i \cdot sc_k^T)}{\exp(\sum_j \sum_{k=1}^{n-1} (sc_n^j \cdot sc_k^T))}, \quad (8)$$

unveils how the scene embedding vectors, which include the concatenation of the visual and text part of a scene, play a key role in the contrastive selection of the optimal denoising process to depict step n of the current sequence. This approach simplifies the overall process and enhances efficiency in terms of new parameters.

3.6 Contrastive Training

During the contrastive selection training phase, we fine-tuned the model to learn non-linear sequential step-to-step relationships. This entailed providing the model with a set of N steps, each originating from a distinct task within a pool of M tasks. Crucially, the input context incorporated the preceding steps for all steps included in the query set,

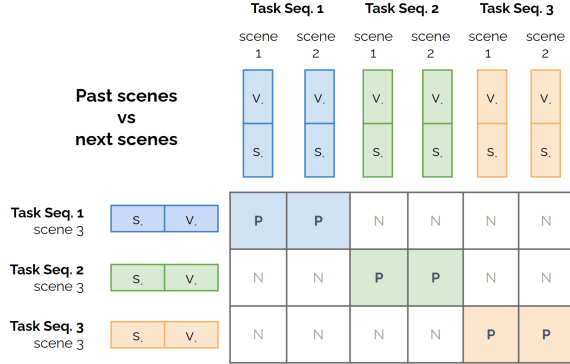


Figure 3: Multi-scene V&L contrastive learning uses multiple sequences a cross-entropy loss guides the model to learn the best next scene according to the ground-truth scenes.

enabling the model to leverage sequential information (see Figure 3). Formally, we adopted the cross-entropy loss function,

$$\arg \min_{w_*} \sum_t^M \sum_{k=1}^N l_{t,k} \log \sigma_{CoSeD}(v_n^j, s_n) \quad (9)$$

to guide the learning process, by comparing the model’s predictions $\sigma_{CoSeD}(\cdot)$ with one-hot encoded ground truth labels $l_{t,k}$ for each task t and step k . These ground truth labels indicate whether a specific step belonged to a task represented in the context.

4 Experimental Setting

Dataset. We collected a dataset consisting of publicly available manual tasks in the recipes domain from [AllRecipes](#) and DIY manual tasks from [WikiHow](#), in an out-of-domain evaluation. Each manual task has a title, a description, a list of ingredients/resources and tools, and a sequence of step-by-step instructions, which may or may not be illustrated. Details about the dataset are in annex A.

Video Diffusion Backbone Models. We experimented CoSeD with Stable Video Diffusion (Blattmann et al., 2023a) and Lumiere (Bar-Tal et al., 2024) models for multi-scene video generation. Testing with both methods evidences the generalization of the method. The choice of Stable Video Diffusion is based on its public availability and Lumiere due to its ability to depict motion.

Baselines. To evaluate CoSeD’s effectiveness in generating coherent image and video sequences for real-world manual tasks, we compared its performance against existing approaches: TALC (Bansal

et al., 2024) with ModelScope (Wang et al., 2023a) and with Lumiere (Bar-Tal et al., 2024), SD 2.1 (Rombach et al., 2022) with Stable Video Diffusion (Blattmann et al., 2023a), stand-alone Lumiere (Bar-Tal et al., 2024), and for image sequences we tested Gill (Koh et al., 2023) and Seed-LLama (Ge et al., 2023). During the evaluation, we prompted all models to generate a complete task.

Human Evaluation for Consistency. We assessed the performance of the developed method and other baselines using CLIP (Radford et al., 2021). We employed CLIP to evaluate the sequence similarity of each task ($V \mapsto V$), and to evaluate the adherence of the generated image to the given textual descriptions ($T \mapsto V$). This offers a comprehensive assessment of the generated images’ alignment with the intended textual descriptions and their visual coherence across the entire sequence.

Annotations focused on the key criteria essential for assessing models generating coherent multi-scene videos. Annotators were asked to evaluate **Visual Consistency** in terms of entities and background, and **Semantic Consistency** in terms of text alignment to the instructional plan. We also report the overall **Sequence Consistency** as the mean of the two previous measures. See annex C for details.

Automatic Evaluation. We assessed the performance of the developed method and other baselines using CLIP (Radford et al., 2021). We employed CLIP to evaluate the sequence similarity of each task ($V \mapsto V$), and to evaluate the adherence of the generated image to the given textual descriptions ($T \mapsto V$). This offers a comprehensive assessment of the generated images’ alignment with the intended textual descriptions and their visual coherence across the entire sequence.

5 Results and Discussion

5.1 Human evaluation

Multi-Scene Consistency Assessment. Results, as shown in Table 1, indicate that CoSeD + Lumiere outperformed the other methods, achieving the highest score of 53.8. This suggests that the combination of CoSeD with Lumiere is particularly effective. Other methods, such as TALC + ModelScope and TALC + Lumiere, despite achieving great scores in Semantic Consistency showed a below average score on Semantic Consistency which shows a deficit in depicting the descriptions.



Figure 4: Example of an illustration for the recipe domain.

Methods	Video Length	Visual Consist.	Semantic Consist.	Sequence Consist.
CoSeD + Lumiere	20.8	61.7	45.9	53.8
CoSeD + SVD	14.9	60.0	39.0	49.5
TALC + ModelScope	7.4	<u>67.8</u>	23.3	45.6
TALC + Lumiere	5.0	76.9	20.5	48.7
SD + SVD	14.9	51.7	35.0	43.3
Lumiere	20.8	60.0	<u>44.0</u>	<u>51.9</u>

Table 1: Manual evaluation in terms of **Visual Consistency**, **Semantic Consistency** and **Sequence Consistency** according to human evaluation.

Overall, the evaluation results indicate that our model performs well, particularly when combined with Lumiere. The improvement observed when integrating Lumiere with other models like TALC and CoSeD further indicates its noteworthy role as an excellent foundational video diffusion model. In contrast, TALC’s lower scores confirm our approach’s advantage on depicting complex multi-scene tasks.

Videos length. We also report length of the generated videos in Table 1. CoSeD combined with either SVD or Lumiere (CoSeD + SVD and CoSeD + Lumiere) achieves an average video length of around 15 and 21 seconds, respectively. This is significantly longer than TALC-based methods (TALC + ModelScope and TALC + Lumiere) which generate shorter videos, around 7 and 5 seconds on average. A visual inspection of the generated videos clearly indicate that CoSeD successfully depict all steps in the task, whereas TALC, despite being a multi-scene model, cannot achieve it. This

Method	Average Rating
CoSeD +Lumiere	2.9 ± 0.99
Ground-truth	4.5 ± 0.55

Table 2: Human annotation for the comparison of the proposed method with ground-truth scenes.

highlights another key strength of our model. Not only does it generate visually coherent and semantically consistent videos, but it also ensures sufficient video length to comprehensively portray the task.

CoSeD vs Groundtruth. To evaluate the absolute quality of the generated video sequences, human annotators rated each sequence on a scale from 1 to 5, comparing them to ground-truth sequences. Deviations like hallucinated visual artifacts or inconsistent actions significantly affect perceived quality. As shown in Table 2, our method achieves over 64% of the ground-truth score, with ground-truth sequences scoring just 0.5 points below the maximum.

5.2 Automatic evaluation

Complementing the human evaluation, we measured CoSeD’s performance using CLIP metrics (see Table 3). Our model achieved a sequence similarity score ($V \mapsto V$) of 84.8 and a description adherence score ($T \mapsto V$) of approximately 27.1. This outperforms image and video baselines in description adherence. These results indicate that our model excels at generating sequences that are both visually realistic and semantically aligned with text

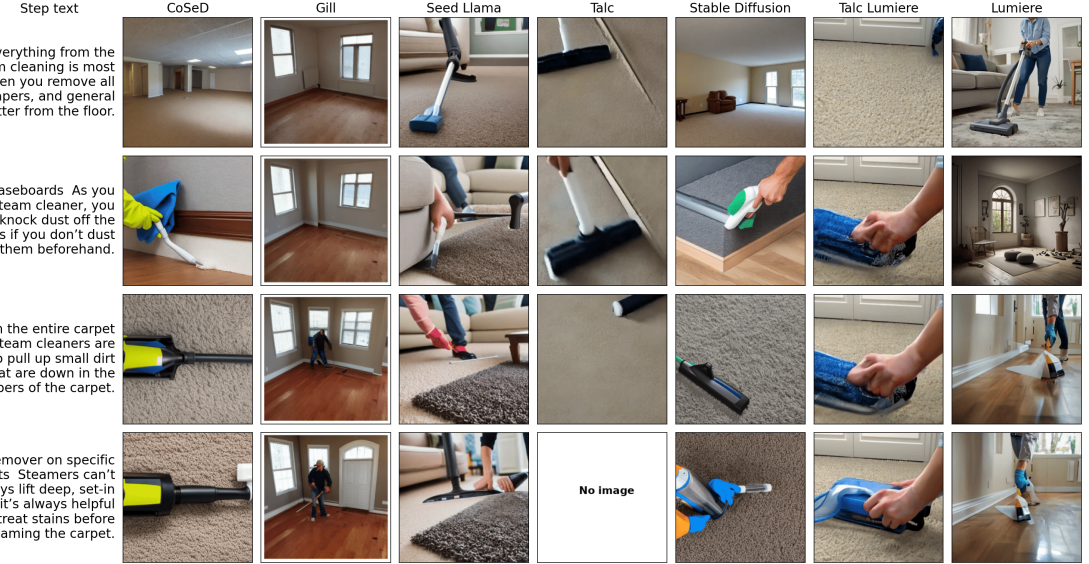


Figure 5: Example of an illustration for the tasks domain.

	Method	$V \mapsto V$	$T \mapsto V$
Image	CoSeD	84.8	27.1
	Seed-Llama	88.0	16.5
	GILL	88.2	22.3
Video	CoSeD + SVD	84.8	27.1
	CoSeD + Lumiere	84.8	27.1
	TALC + ModelScope	81.8	12.4
	TALC + Lumiere	90.7	15.3
	SD + SVD	82.1	26.4
	Lumiere	83.4	14.9

Table 3: Automatic evaluation in terms of CLIP visual similarity ($V \mapsto V$) and CLIP semantic similarity ($T \mapsto V$).

prompts, underscoring its potential for practical applications.

In a comparison to other sequence-generating models (see Table 3), CoSeD with both Video Stable Diffusion and Lumiere consistently achieved the highest description adherence ($T \mapsto V$) without discarding the sequence similarity ($V \mapsto V$).

When comparing CoSeD with the best model in sequence similarity, our model lags by only 5.9% while gains 11.8% in description adherence. While TALC + Lumiere excels in maintaining high sequence similarity, CoSeD demonstrates superior description adherence without compromising sequence similarity. This strong description adherence score highlights our model’s effectiveness in aligning generated content with text descriptions,

which is crucial for tasks such as accurately converting textual descriptions into videos. Compared to vanilla video-only models, our approach surpasses both metrics, leading to improved results.

5.3 Qualitative Analysis

Figure 4 provides a closer look at how different methods influence the quality of generated videos and image sequences for a certain recipe. Our model excels in maintaining a consistent background, keeping the same pan, and ensuring the ingredients evolve seamlessly from raw to final recipe. This accurate depiction of sequence provides a visually stable and easy-to-follow experience for viewers.

Regarding the out-of-scope diy task in Figure 5 our model can depict larger actions such as showing a room without furniture or the action of cleaning a baseboard. Nonetheless, it has some difficulties depicting complex tools like a vacuum cleaner. Other methods tend to focus on the bigger picture, failing to depict the task itself accurately or omitting steps altogether, as seen with TALC.

5.4 Ablation Studies

In this section, we inspect the influence of latent variables and how CoSeD selects the optimal denoising iteration latent and the denoising step of the complete sequence.

Denoising latents. Understanding the influence of latent variables on the coherence and fidelity of generated sequences is crucial for refining our

model. To this end, we assess how various latent selections affect step coherence and textual description adherence. Figure 6 shows a clear correlation between latent settings and the model’s ability to generate coherent and textually aligned sequences.

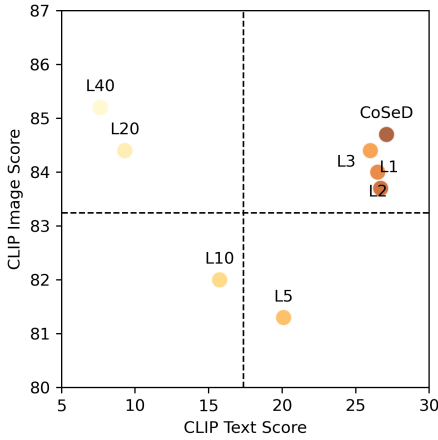


Figure 6: Impact of denoising latents in the performance of CoSeD’s visual and semantic similarity.

The analysis of CLIP scores in Figure 6 categorizes latent configurations into four key areas. The ideal zone features configurations excelling in both sequence similarity (high CLIP Image Score) and description adherence (high CLIP Text Score). CoSeD, which leverages a set of latent configurations, achieves this balance, demonstrating its ability to generate clear, informative, and visually consistent video sequences. In addition, configurations with Latent 5 show moderate text adherence but lack visual coherence, potentially leading to nonsensical sequences. In contrast, latents 20 and 40 generate visually similar images with high coherence, but these images deviate significantly from the intended task steps, leading to poor text adherence. These configurations tend to generate images that are normally just blurry and too similar to each other, as detailed in Annex F. Lastly, configurations like Latent 10 exhibit minimal success in both visual coherence and text alignment. Understanding this relationship between latent configurations and CLIP scores is crucial for achieving high-quality video generation.

Finally, we can see that CoSeD (top-right mark) is leveraging the performance of all denoising latents used – the contrastive selection of the denoising latents leads to a performance that is higher than with the individual latents.

Denoising latents + Denoising steps. As we observed in the previous section, latents 1 to 3 hold most of the information. However, a key property of CoSeD is its ability to assess the full sequence of denoising steps and the denoising iterations of each step. The sequential generation involves building upon previous steps, but the direct relationship between these steps varies according to the contrastive property of CoSeD, as illustrated in Figure 7.

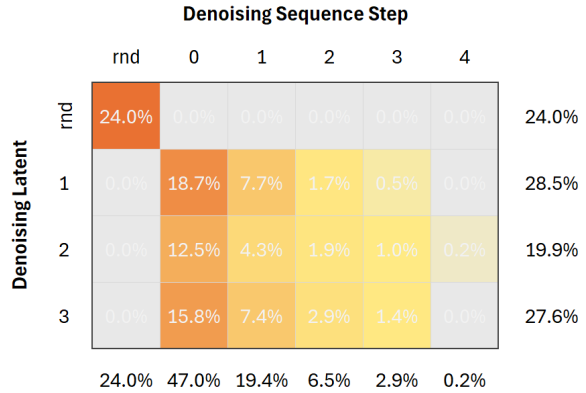


Figure 7: The average number of times that CoSeD selected a given step/latent to generate the next scene.

Contrary to expectations that the model would primarily focus on the latents from the preceding step, Figure 7 demonstrates that the most relevant information may actually reside in earlier steps rather than the immediately preceding one. This highlights the importance latent selection as an integral part of the video generation process, influencing CoSeD’s ability to produce clear, grounded and coherent multi-scene content.

6 Conclusion

In this paper we propose CoSeD, a contrastive sequential-denoising method to generate multi-scene videos. The method examines all steps simultaneously to ensure an optimal consistency between the new scene and all previous scenes. Additionally, the compact size of our model facilitates efficient training, enabling domain specific fine-tuning. An interesting property of CoSeD, is its model-independent nature, supporting ensembles of diffusion models for optimal results.

The consistent gains obtained in real-world depictions of sequences of actions, supports our initial hypothesis and highlights the need to deepen our understanding of denoising latents in multi-scene and sequence settings.

7 Limitations and Risks

While we conducted a comprehensive set of experiments and validations, there are other experiments and additional research that can provide further insights into several aspects of the proposed method. Firstly, we did not investigate the potential benefits of using mixtures of latents or considering random images as candidates for each step. Secondly, CoSeD supports heterogeneous video diffusion methods, which we did not experiment. Thirdly, we did not explore the effects of using a larger LLM with prompting.

Approaches such as those demonstrated in previous works (Long et al., 2024; Lin et al., 2023) leverage both background and foreground information from similar reference images to generate the next scene.

References

Hritik Bansal, Yonatan Bitton, Michal Yarom, Idan Szpektor, Aditya Grover, and Kai-Wei Chang. 2024. **Talc: Time-aligned captions for multi-scene text-to-video generation.** *Preprint*, arXiv:2405.04682.

Omer Bar-Tal, Hila Chefer, Omer Tov, Charles Hermann, Roni Paiss, Shiran Zada, Ariel Ephrat, Jun-hwa Hur, Yuanzhen Li, Tomer Michaeli, Oliver Wang, Deqing Sun, Tali Dekel, and Inbar Mosseri. 2024. **Lumiere: A space-time diffusion model for video generation.** *Preprint*, arXiv:2401.12945.

Andreas Blattmann, Tim Dockhorn, Sumith Kulal, Daniel Mendelevitch, Maciej Kilian, Dominik Lorenz, Yam Levi, Zion English, Vikram Voleti, Adam Letts, Varun Jampani, and Robin Rombach. 2023a. **Stable video diffusion: Scaling latent video diffusion models to large datasets.** *CoRR*, abs/2311.15127.

Andreas Blattmann, Robin Rombach, Huan Ling, Tim Dockhorn, Seung Wook Kim, Sanja Fidler, and Karsten Kreis. 2023b. **Align your latents: High-resolution video synthesis with latent diffusion models.** In *IEEE/CVF Conference on Computer Vision and Pattern Recognition, CVPR 2023, Vancouver, BC, Canada, June 17-24, 2023*, pages 22563–22575. IEEE.

João Bordalo, Vasco Ramos, Rodrigo Valerio, Diogo Glória-Silva, Yonatan Bitton, Michal Yarom, Idan Szpektor, and João Magalhães. 2024. **Generating coherent sequences of visual illustrations for real-world manual tasks.** *CoRR*, abs/2405.10122.

Lucia Donatelli, Theresa Schmidt, Debanjali Biswas, Arne Köhn, Fangzhou Zhai, and Alexander Koller. 2021. **Aligning actions across recipe graphs.** In *Proceedings of the 2021 Conference on Empirical Methods in Natural Language Processing*, pages 6930–6942, Online and Punta Cana, Dominican Republic. Association for Computational Linguistics.

Zhangyin Feng, Yuchen Ren, Xinmiao Yu, Xiaocheng Feng, Duyu Tang, Shuming Shi, and Bing Qin. 2023. **Improved visual story generation with adaptive context modeling.** In *Findings of the Association for Computational Linguistics: ACL 2023*, pages 4939–4955, Toronto, Canada. Association for Computational Linguistics.

Yuying Ge, Sijie Zhao, Ziyun Zeng, Yixiao Ge, Chen Li, Xintao Wang, and Ying Shan. 2023. **Making llama SEE and draw with SEED tokenizer.** *CoRR*, abs/2310.01218.

Patrizia Grifoni. 2009. *Multimodal human computer interaction and pervasive services*. IGI Global.

Jonathan Ho, William Chan, Chitwan Saharia, Jay Whang, Ruiqi Gao, Alexey A. Gritsenko, Diederik P. Kingma, Ben Poole, Mohammad Norouzi, David J. Fleet, and Tim Salimans. 2022. **Imagen video: High definition video generation with diffusion models.** *CoRR*, abs/2210.02303.

Jing Yu Koh, Daniel Fried, and Russ Salakhutdinov. 2023. **Generating images with multimodal language models.** In *Advances in Neural Information Processing Systems 36: Annual Conference on Neural Information Processing Systems 2023, NeurIPS 2023, New Orleans, LA, USA, December 10 - 16, 2023*.

Dongxu Li, Junnan Li, Hung Le, Guangsen Wang, Silvio Savarese, and Steven C. H. Hoi. 2022. **Lavis: A library for language-vision intelligence.** *Preprint*, arXiv:2209.09019.

Angela Lin, Sudha Rao, Asli Celikyilmaz, Elnaz Nouri, Chris Brockett, Debadatta Dey, and Bill Dolan. 2020. **A recipe for creating multimodal aligned datasets for sequential tasks.** In *Proceedings of the 58th Annual Meeting of the Association for Computational Linguistics*, pages 4871–4884, Online. Association for Computational Linguistics.

Han Lin, Abhay Zala, Jaemin Cho, and Mohit Bansal. 2023. **Videodirectorgpt: Consistent multi-scene video generation via llm-guided planning.** *CoRR*, abs/2309.15091.

Fuchen Long, Zhaofan Qiu, Ting Yao, and Tao Mei. 2024. **Videodrafter: Content-consistent multi-scene video generation with LLM.** *CoRR*, abs/2401.01256.

Adyasha Maharana, Darryl Hannan, and Mohit Bansal. 2022. **Storydall-e: Adapting pretrained text-to-image transformers for story continuation.** In *Computer Vision – ECCV 2022: 17th European Conference, Tel Aviv, Israel, October 23–27, 2022, Proceedings, Part XXXVII*, page 70–87, Berlin, Heidelberg. Springer-Verlag.

OpenAI. 2023. **GPT-4** technical report. *CoRR*, abs/2303.08774.

Xichen Pan, Pengda Qin, Yuhong Li, Hui Xue, and Wenhui Chen. 2022. **Synthesizing coherent story with auto-regressive latent diffusion models**. *CoRR*, abs/2211.10950.

Alec Radford, Jong Wook Kim, Chris Hallacy, Aditya Ramesh, Gabriel Goh, Sandhini Agarwal, Girish Satsky, Amanda Askell, Pamela Mishkin, Jack Clark, Gretchen Krueger, and Ilya Sutskever. 2021. **Learning transferable visual models from natural language supervision**. *Preprint*, arXiv:2103.00020.

Tanzila Rahman, Hsin-Ying Lee, Jian Ren, Sergey Tulyakov, Shweta Mahajan, and Leonid Sigal. 2023. **Make-a-story: Visual memory conditioned consistent story generation**. In *IEEE/CVF Conference on Computer Vision and Pattern Recognition, CVPR 2023, Vancouver, BC, Canada, June 17-24, 2023*, pages 2493–2502. IEEE.

Robin Rombach, Andreas Blattmann, Dominik Lorenz, Patrick Esser, and Björn Ommer. 2022. **High-resolution image synthesis with latent diffusion models**. In *IEEE/CVF Conference on Computer Vision and Pattern Recognition, CVPR 2022, New Orleans, LA, USA, June 18-24, 2022*, pages 10674–10685. IEEE.

Frank Serafini. 2014. *Reading the visual: An introduction to teaching multimodal literacy*. Teachers College Press.

Uriel Singer, Adam Polyak, Thomas Hayes, Xi Yin, Jie An, Songyang Zhang, Qiyuan Hu, Harry Yang, Oron Ashual, Oran Gafni, Devi Parikh, Sonal Gupta, and Yaniv Taigman. 2023. **Make-a-video: Text-to-video generation without text-video data**. In *The Eleventh International Conference on Learning Representations, ICLR 2023, Kigali, Rwanda, May 1-5, 2023*. OpenReview.net.

Jiuniu Wang, Hangjie Yuan, Dayou Chen, Yingya Zhang, Xiang Wang, and Shiwei Zhang. 2023a. **Modelscope text-to-video technical report**. *arXiv preprint arXiv:2308.06571*.

Yaohui Wang, Xinyuan Chen, Xin Ma, Shangchen Zhou, Ziqi Huang, Yi Wang, Ceyuan Yang, Yinan He, Jiashuo Yu, Peiqing Yang, Yuwei Guo, Tianxing Wu, Chenyang Si, Yuming Jiang, Cunjian Chen, Chen Change Loy, Bo Dai, Duhua Lin, Yu Qiao, and Ziwei Liu. 2023b. **LAVIE: high-quality video generation with cascaded latent diffusion models**. *CoRR*, abs/2309.15103.

Shengming Yin, Chenfei Wu, Huan Yang, Jianfeng Wang, Xiaodong Wang, Minheng Ni, Zhengyuan Yang, Linjie Li, Shuguang Liu, Fan Yang, Jianlong Fu, Ming Gong, Lijuan Wang, Zicheng Liu, Houqiang Li, and Nan Duan. 2023. **NUWA-XL: diffusion over diffusion for extremely long video generation**. In *Proceedings of the 61st Annual Meeting of the Association for Computational Linguistics (Volume 1: Long Papers), ACL 2023, Toronto, Canada, July 9-14, 2023*, pages 1309–1320. Association for Computational Linguistics.

Zhengqing Yuan, Ruoxi Chen, Zhaoxu Li, Haolong Jia, Lifang He, Chi Wang, and Lichao Sun. 2024. **Mora: Enabling generalist video generation via a multi-agent framework**. *Preprint*, arXiv:2403.13248.

Yupeng Zhou, Daquan Zhou, Ming-Ming Cheng, Jiashi Feng, and Qibin Hou. 2024. **Storydiffusion: Consistent self-attention for long-range image and video generation**. *Preprint*, arXiv:2405.01434.

A Dataset

We compiled a dataset consisting of publicly available manual tasks from the recipes domain sourced from [AllRecipes](#). Additionally, we included DIY manual tasks from [WikiHow](#) for an out-of-domain evaluation.

Each task in the dataset includes a title, a description, a list of ingredients/resources and tools, and a sequence of step-by-step instructions, which may or may not be illustrated. To facilitate the illustration of task steps, we focused on tasks that are mostly illustrated, allowing us to use these images as ground truth for training and evaluating our methods.

The dataset comprises approximately 1,400 tasks, with an average of 4.9 steps per task, amounting to a total of 6,860 individual steps. Most tasks include an image for each step, and some feature a complete recipe video that is segmented into multiple clips, with each clip lasting between 10 and 30 seconds per step.

Considering that the number of illustrations can impact accuracy, we limited the training tasks to those with no more than 10 steps.

B Model Training

We opted for the CLIP model with a patch size of 32 to serve as the encoder for both image and text data due to its reputation in effectively capturing visual and textual information. In training our own architecture, we conducted experiments with various hyperparameters, including different learning rates, learning rate schedulers, dropout rates, layer freezing, and batch sizes, in order to identify the most suitable settings for our specific problem.

For the loss function, we employed cross-entropy, comparing the softmax output with hot-encoding of the steps that belong to each task. It's important to note that while this loss function indicates step-task associations, it may not always accurately reflect the model's overall performance on the task at hand. During the tuning of hyperparameters, we found that freezing layers, weight decay, dropout, and learning rate schedulers had minimal impact on model performance.

The best model, which has about 600,000 parameters, was refined using specific training parameters listed in Table 4. Training was completed in under two minutes, utilizing an A100-40GB GPU and spanning across ten epochs. Employing the Cross-Entropy loss function, the training process operated

Training Details	
Optimizer	Adam
Loss Function	Cross-Entropy
Batch Size	500
Learning Rate	0.01
Epochs	10
Model Max Length	400
Number of GPUs	1 A100-40GB

Table 4: Training parameters

with a batch size of 500 and a learning rate set at 0.01, using the Adam optimizer.

Single Modalities. In multimodal generation tasks, the integration of different modalities can significantly impact the final output. Through this ablation study, we explore the implications of using singular modalities—text, images, or perturbed inputs—and examine the importance of modality mixing for enhancing generation quality.

Initially, in the scenario where text remains static across inputs, the model struggles with adaptability and generalization due to its reliance on a singular textual context. Conversely, when all inputs are randomized, the absence of consistent patterns across modalities impedes the model's learning process, resulting in suboptimal performance. However, the configuration where only text is randomized exhibits superior performance, suggesting that the model relies more on image over text. Notably, the marginal difference in performance between random text and the standard training approach underscores the intricate nature of multimodal tasks.

Our analysis underscores the importance of modality mixing in enhancing multimodal generation tasks. Integrating multiple modalities empowers the model to leverage diverse information sources, leading to more nuanced and accurate outputs. In conclusion, the complexity of multimodal data shows that a model can rely more on one modality over the other but a mix of both will always be a better conjunction over a single modality.

Prompt Rewriter Training The training process was centred on enabling the Large Language Model (LLM) to function as a visual caption generator for original task steps. Leveraging the capabilities of InstructBLIP (Li et al., 2022), we created contextual captions corresponding to each image and its associated step within the dataset. By integrating

relevant task context into the generation of ground truth data, we enhanced the LLM’s performance for visual clues. This approach ensured the production of accurate and contextually aligned visual descriptions, solidifying its role as an adept image caption generator.

C Human annotations

In Figure 8, we display the screenshot used for human evaluation on Amazon Mechanical Turk. Annotators were tasked with assessing the visual quality, entity consistency, background consistency, and adherence to text of the multi-scene generated videos across various task prompts and scene quantities.

C.1 Annotations Job

Participants for this evaluation were recruited through the crowdsourcing platform Amazon Mechanical Turk. Annotators were compensated at a rate of \$0.5 per task, and each task was designed to take between 2 and 3 minutes to complete.

The payment rate of \$0.5 per task was determined based on pilot tests to estimate the average time required for completion and to ensure fair compensation for participants’ time and effort. At this rate, annotators could earn approximately \$10 per hour if tasks were completed consistently within 3 minutes each, which exceeds the current federal minimum wage in the United States.

All annotators were aware that they were collaborating with researchers for an evaluation on video generation. They received detailed information about their tasks and how their evaluations would contribute to the research.

With focus on the task itself, we maintained annotators’ anonymity. Consequently, we do not have specific demographic or geographic information about the annotator population that provided the data for this study.

C.2 Annotation Process

The annotation process consisted of three main steps:

1. **Instruction Phase:** Annotators received a slideshow with detailed instructions on how to perform the annotations. This phase included several examples to train the annotators and ensure clarity regarding the task requirements.
2. **Qualification Phase:** After the instruction phase, annotators completed a qualification

task involving five example annotations. This step was designed to assess their understanding and ability to perform the tasks according to our standards. Only those who passed this qualification phase proceeded to the final annotation phase.

3. **Annotation Phase:** Qualified annotators were then given the full set of annotation tasks, where they evaluated the final results.

C.3 Annotation Tasks

The human annotation pool consisted of annotators who successfully passed the qualification phase.

Figure 8 illustrates the task layout for selecting the best visual coherence maintaining method. Annotators evaluated six models: *CoSeD + Stable Video Diffusion*, *CoSeD + Lumiere*, *TALC + ModelScope*, *TALC + Lumiere*, *Lumiere*, and *Stable Diffusion + Stable Video Diffusion*. They graded the videos on visual quality, entity consistency, background consistency, and adherence to text.

Figure 9 outlines the annotation guidelines for evaluating the sequences generated by our method compared to other baselines. This figure provides detailed criteria for the annotators to follow, ensuring consistency in their assessments.

In Figure 10, the specific task of rating sequences generated by our method against ground-truth images is depicted. Annotators were asked to score these sequences on a scale from 1 to 5, providing a quantitative measure of our model’s performance.

To complement this, Figure 11 presents the detailed guidelines used for rating sequences generated by our method compared to ground-truth images. These guidelines helped standardize the evaluation process, ensuring that the ratings were fair and consistent across different annotators.

The results from the human annotations provide valuable insights into the performance of different models across the specified criteria. Detailed feedback from annotators helps in understanding the strengths and weaknesses of our model, guiding future improvements.

D Prompt Optimization

We attempted to enhance generation quality by refining our prompts, incorporating detailed descriptions. These descriptions included:

- **Main Subject:** Highlighting the primary focus of the image, whether it’s ingredients in a recipe or materials for a project.

Answer the following questions based on the multiple-scene descriptions and the candidate generated video.



Descriptions:

Scene 1. Heat the Coconut Oil in a wide pan over a medium flame, then add the Onion, Garlic, Scallion, and Ground Black Pepper. Reduce the heat to low for about 3-4 minutes.
Scene 2. Add the Small Shrimp, stir well and cook for another 3 minutes.
Scene 3. Turn the heat up to medium high and add the Jamaican Callaloo, Tomato, Scotch Bonnet Pepper, Fresh Thyme, and Sea Salt. After a couple minutes, add the Water and cook until tender.
Scene 4. After about 10-12 minutes, taste for salt and adjust accordingly.

Does the video **scene** exhibit a good **Visual Quality**? (are there any disappearing objects, deformed objects and undesirable artifacts in the video?)
 Yes Partially No

Does the video exhibit **Entity Consistency** between **scenes**? (entities are consistent e.g., the shape and features of the objects do not change unless specified)
 Yes Partially No

Does the video exhibit **Background Consistency** between **scenes**? (background is consistent when required e.g., the tool does not change without a change described in the scene description)
 Yes Partially No

Does the video exhibit **Text Adherence**? (each **scene** is aligned with the textual description)
 Yes Partially No

Submit

Figure 8: Human Annotation Layout for Video Generation Methods

- **Item:** Encompassing all inanimate objects, ranging from everyday items like utensils or tools to more abstract entities like machinery.
- **Setting:** Depicting the broader environment or backdrop, spanning from kitchen countertops to workshop benches or outdoor landscapes.
- **Activity:** Illustrating dynamic actions or steps that animate the imagery, such as stirring ingredients or assembling components.
- **Feeling:** Conveying the emotional resonance elicited by the image, whether it evokes joy, satisfaction, anticipation, or other sentiments.
- **Arrangement:** Describing the spatial layout, indicating how elements are positioned relative to each other, like 'stacked neatly' or 'arranged in a circular pattern.'

In the end, though, these prompts failed to produce better outcomes.

E Selecting the First Image

In the process of generating visual representations based on textual input, the selection of the initial image or video is crucial. This selection not only serves as the first interaction with the user but also influences subsequent representations, directly impacting the overall quality of the generated content. Therefore, establishing a robust strategy for selecting the first image is essential to ensure coherence and effectiveness in the generated output.

The significance of the initial image choice lies in its potential to enhance user engagement. A mismatch between the text and visual representation can disrupt comprehension and decrease the overall user experience. Therefore, the selection strategy should consider factors such as alignment with the text, diversity, and relevance to ensure a seamless transition from text to visuals.

Single Image Generation. This strategy offers simplicity and directness as its main advantages. By generating a single image, it provides a straightforward solution without added complexity. However, it may suffer from a lack of variety, potentially resulting in limited diversity in the initial representation. Additionally, its reliance on the Stable Diffusion model's capabilities means that the quality and text adherence of the generated image depends solely on the model's performance.

Random Selection from Image Batch. The random selection strategy offers increased diversity and reduced bias. By allowing the selection of a random image from a batch, it potentially offers a wider range of visual representations. Moreover, it avoids intentional or unintentional bias in selecting the first image. However, it lacks control over the selection process, which may lead to the choice of an image that does not align well with the text. Furthermore, the quality and relevance of the selected image may vary across different runs, introducing potential inconsistency.

Using CLIP for Selection. In this approach, CLIP is used to meticulously select the initial image based on its semantic similarity to the textual

Instructions

1. Watch the entire video provided on the left side of the screen.
2. Carefully read the descriptions provided on the right side of the screen.
3. Evaluate the video based on the following criteria:
 - **Visual Quality:** Check if the video scene has good visual quality without any disappearing or deformed objects and no undesirable artifacts.
 - **Entity Consistency:** Ensure that the entities (objects) are consistent between scenes, with no unexpected changes unless specified in the descriptions.
 - **Background Consistency:** Confirm that the background remains consistent between scenes, unless a change is described in the scene description.
 - **Text Adherence:** Verify that each scene in the video aligns with the corresponding textual description.
4. Select the appropriate answer for each question below the video and descriptions.
5. Double-check your answers before submitting the form.

Figure 9: Instructions for Video Generation Evaluation

Rate the video based on the provided descriptions.



Descriptions:
Scene 1. Dice chicken breasts into large pieces. Mince garlic and cilantro, cut bell peppers into strips, and finely chop scallions.
Scene 2. Heat half of the vegetable oil in a large skillet over high heat. Add chicken pieces and sauté for approx. 5 – 7 min. until golden. Transfer to a plate and set aside.
Scene 3. Heat other half of vegetable oil and add scallions and garlic. Sauté until soft and fragrant for approx 1 - 2 min. Then, add bell pepper. Continue to sauté and add corn, chicken stock, and enchilada sauce. Season with salt and pepper.
Scene 4. Bring to a simmer and add rice. Cover and cook on medium-low heat for approx. 15 min. for white rice and 30 min. for brown rice until rice is al dente and most of the liquid absorbed. Preheat oven to 180°C/350°F and turn on the top heat, or set the broiler to high.
Scene 5. Shred chicken and combine with rice. Spread cheese on top, place skillet in the oven, and broil for approx. 5 - 10 min., or until cheese begins to melt. Garnish with cilantro and

Rate the overall quality of the video considering all the mentioned criteria (1 being the lowest and 5 being the highest):
 1 2 3 4 5

Submit

Figure 10: Human Annotation Layout for Our Method vs. Ground Truth

description. By leveraging CLIP’s robust understanding of semantics, we ensure that the chosen image corresponds well with the text, thereby enhancing both coherence and relevance. Importantly, the computational overhead associated with CLIP is minimal compared to the resource-intensive task of image generation. Unlike other options, utilizing CLIP for image selection notably increases the likelihood of achieving coherence and relevance in the first generated content.

Selecting the first image during the generation of visual representations from sequential text input is a critical step. Among the presented strategies for selecting the initial image, the approach of using CLIP for selection stands out as the most promising. This strategy emphasizes semantic alignment,

ensuring coherence and relevance between the text and visual representation. By leveraging CLIP’s capabilities, we aim to enhance the overall quality and effectiveness of the generated output.

F Latent Selection Example

This annex provides an example of different latents used to depict the same step. It is evident that the image quality decreases as the latent value increases. With higher latent values, the images become more similar to each other, which can increase the image similarity score but decrease the text adherence of the generated images.

Instructions

We will present you with a video clip representing a sequence of steps.

Your task is to rate the video on a scale of 1-5 based on the following factors:

- **Representation of Instructions:** How well does the video illustrate the given instructions?
 - *Note:* Any generation artifacts should not impact the rating if the overall video clearly conveys the steps.
- **Coherence:** How coherent is the sequence of scenes in the video?
 - *Example:* If an object is blue in one scene, it should remain blue in subsequent scenes.
 - *Example:* The background should remain consistent across the video.

Figure 11: Instructions for Ground Truth Annotation



Figure 12: CLIP Selection



Figure 13: Using different latents for image generation

G Generation Examples

In the following pages, we present several examples of video keyframes and image sequences generated to illustrate specific tasks such as do-it-yourself and recipes using our method and the baselines.

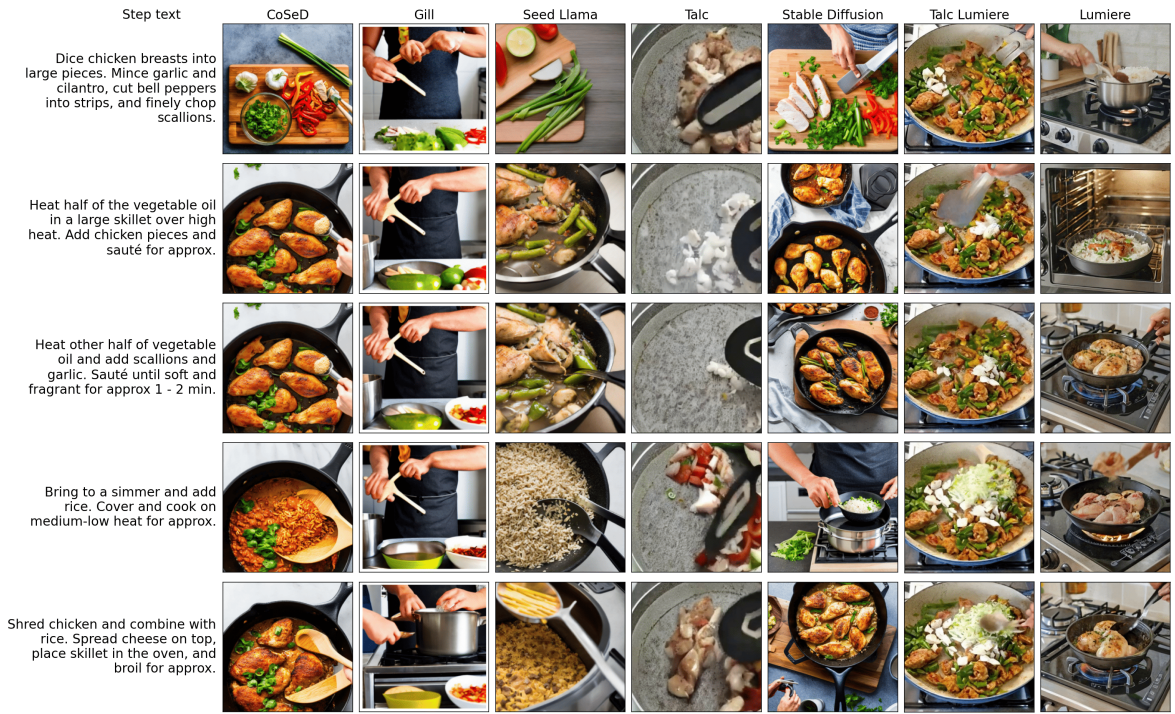


Figure 14: Example of generation with the baselines.

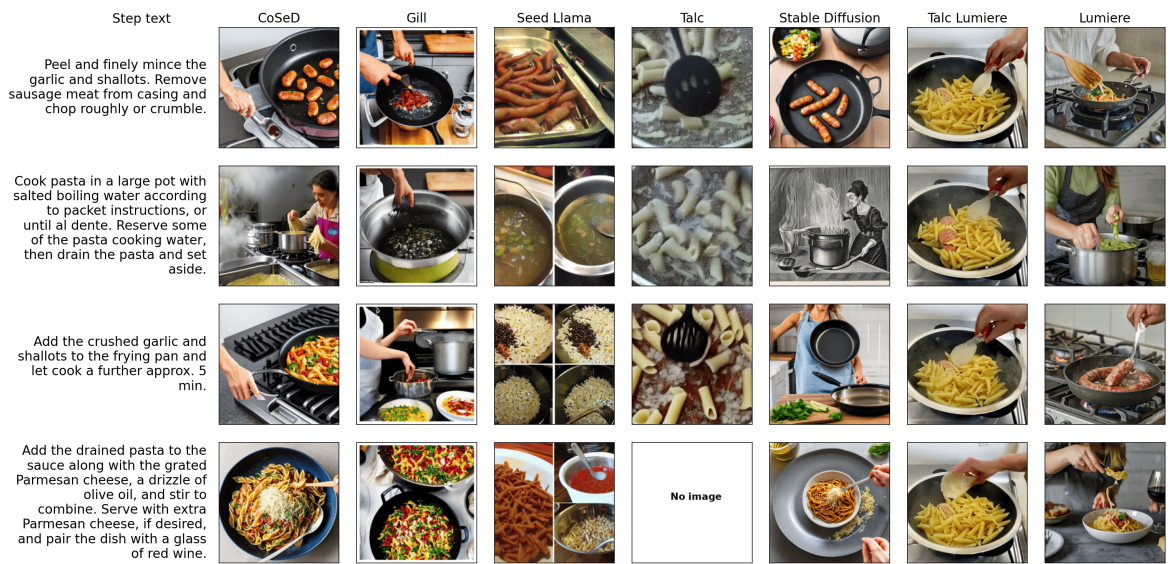


Figure 15: Example of generation with the baselines.



Figure 16: Example of generation with the baselines.



Figure 17: Example of generation with the baselines.

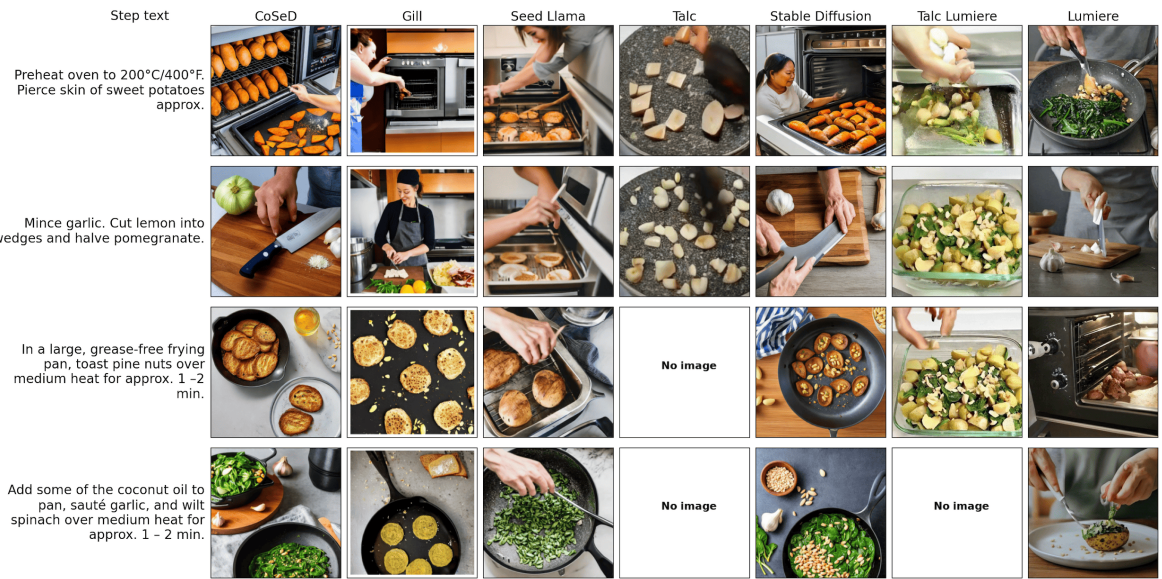


Figure 18: Example of generation with the baselines.



Figure 19: Example of generation with the baselines.



Figure 20: Example of generation with the baselines.

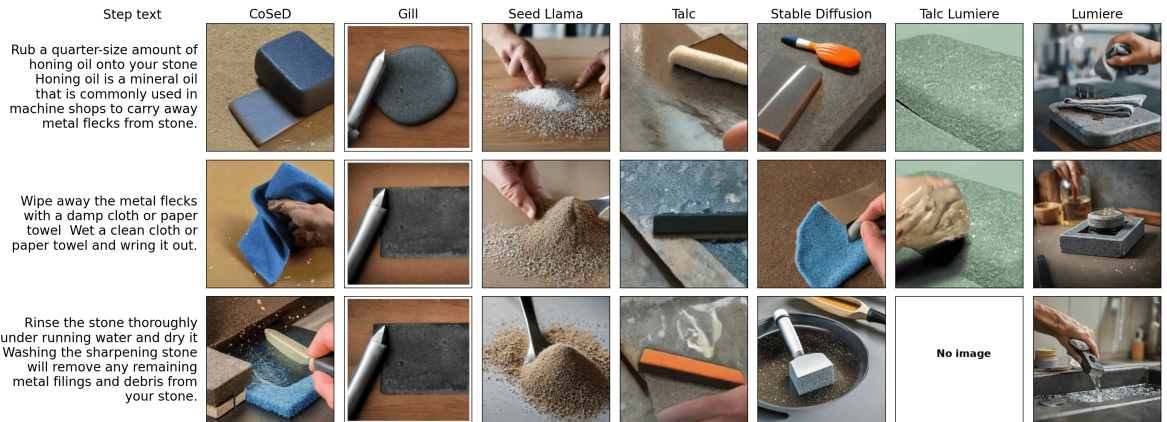


Figure 21: Example of generation with the baselines.



Figure 22: Example of generation with the baselines.

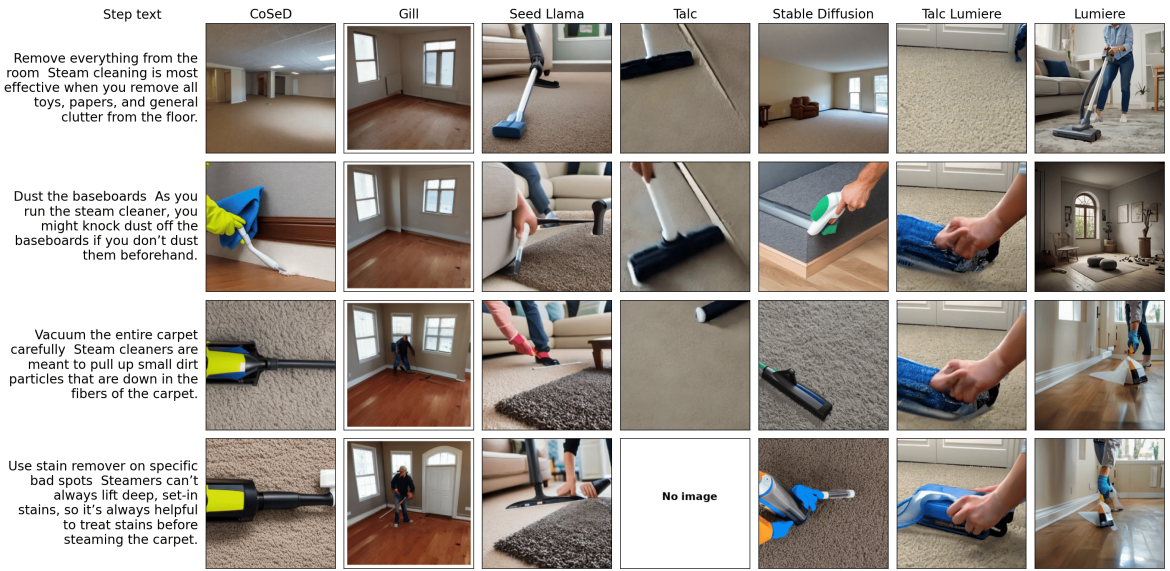


Figure 23: Example of generation with the baselines.

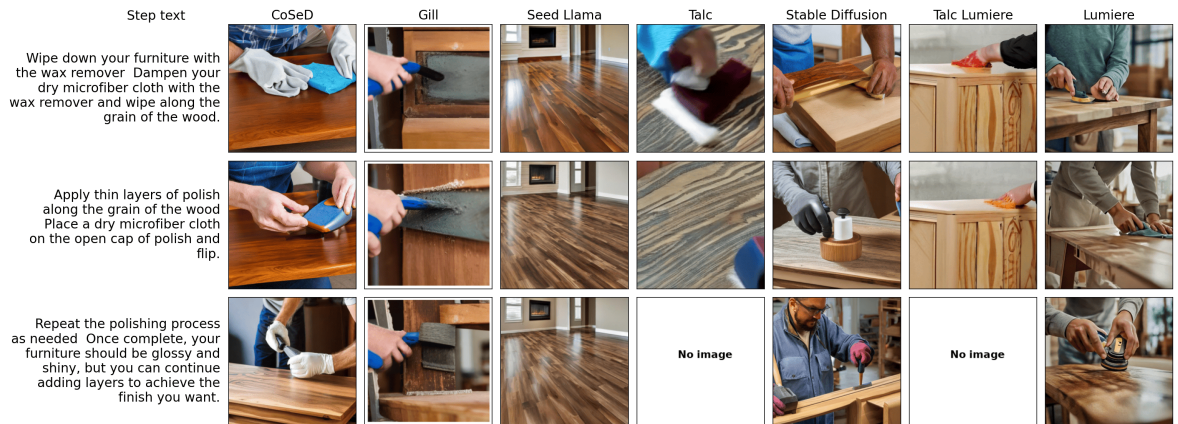


Figure 24: Example of generation with the baselines.